Original Article
Inhibition of HIF-1α by PX-478 suppresses tumor growth of esophageal squamous cell cancer in vitro and in vivo

Yingming Zhu[1*], Yuanwei Zang[2*], Fen Zhao[1], Zhenxiang Li[1], Jianbo Zhang[3], Liang Fang[2], Minghuan Li[1], Ligang Xing[1], Zhonghua Xu[2], Jinming Yu[1]

*Departments of [1]Radiation Oncology, [3]Pathology, Shandong Cancer Hospital and Institute, Shandong University, Jinan, China; [2]Department of Urology, Qilu Hospital, Shandong University, Jinan, China. *Equal contributors.*

Abstract: The aim of this study is to investigate the clinical significance of hypoxia inducible factor-1α (HIF-1α) expression in esophageal squamous cell cancer (ESCC) and clarify the effects of PX-478, a selective HIF-1α inhibitor, on ESCC both in vitro and in vivo. HIF-1α, cyclooxygenase-2 (COX-2) and programmed death ligand-1 (PD-L1) were markedly overexpressed in ESCC tissue and associated with poorer survival. In vitro, both COX-2 and PD-L1 expression of ESCC cells were significantly induced by $CoCl_2$ treatment, but inhibited by HIF-1α knock-down or PX-478 treatment. Furthermore, PX-478 significantly inhibited tumor cell proliferation by inhibiting the G2/M transition and promoting apoptosis of ESCC cells. In addition, inhibited epithelial-mesenchymal transition was observed after PX-478 treatment. In vivo, PX-478 significantly decreased tumor volume following subcutaneous implantation. Together, our results indicated that PX-478 had significant antitumor activity against HIF-1α over-expressing ESCC tumors in vitro and in vivo. These results opened up the possibility of inhibiting HIF-1α for targeted therapy of ESCC.

Keywords: Esophageal squamous cell cancer (ESCC), hypoxia inducible factor-1α (HIF-1α) inhibitors, PX-478, tumor growth, epithelial-mesenchymal transition (EMT)

Introduction

Esophageal cancer (EC) is identified as one of the leading causes of cancer death in China [1]. The main histological subtype of the disease, esophageal squamous cell cancer (ESCC), is particularly prevalent in Asia and Africa [2, 3]. Despite the latest innovations in ESCC treatment, long-term survival remains poor. Overall 5-year survival rate is only 20% and the majority of patients will relapse [2]. Thus, it is important to develop novel molecular targets and therapeutic strategies in ESCC.

Quite different prognosis existed in middle stage patients in ESCC, which can be good materials for further research into novel molecular targets [4]. Patients of pathological stage T3N0M0 (pT3N0M0) were divided into stages IB, IIA, and IIB in the new staging system (7th edition) of the American Joint Committee on Cancer (AJCC) [4]. In this study, we concentrated on this small portion of patients to find

some prognostic markers independently of TNM stage.

Hypoxia, which involves low pressure of oxygen in the tumor microenvironment, is a characteristic of many solid tumors [5]. Hypoxia-inducible factor-1 (HIF-1) is a major transcription factor that regulates cell responses to hypoxia, which comprises an oxygen-sensitive α-subunit (HIF-1α) and a constitutively expressed β-subunit (HIF-1β) [6]. HIF-1α is the functional subunit and is regulated by oxygen levels, while HIF-1β a constitutively expressed nuclear protein [6]. In ESCC, the proportion of high HIF-1α expression ranged from 30.8 to 70.3% in individual studies while very little expression of HIF-1α was found in the normal esophageal epithelium [7, 8]. HIF-1α activates a series of genes, which encode proteins involved in cell proliferation, apoptotic pathway, invasiveness, angiogenesis and metastasis [5]. Among these direct target genes that control the metabolic switch for optimal cellular adaptation to hypoxia, cyclooxygen-

ase-2 (COX-2) has been implicated in carcinogenesis and tumor progression from inflammation [9]. Overexpression of COX-2 has been implicated in the pathogenesis, disease progression and poor survival rates in various tumor types, including ESCC [10]. Another direct target gene of HIF-1α is the immune checkpoint programmed death ligand-1 (PD-L1) [11, 12]. PD-L1, ligand of programmed death 1 (PD-1), is a negative co-stimulatory factor that inhibits T cell activation and is expressed on cancer cells, T cells, macrophages, and dendritic cells and so on [13]. The PD-L1/PD-1 interaction has been found to be associated with poor prognosis and clinical outcomes in various cancers [14]. Although Immune checkpoint-blocking agents directed at this interaction have been clinically successful, very few people in developing countries can afford the prohibitive expense. As an important mediator and regulator of gene expression patterns, HIF-1α could be a new effective means of controlling ESCC.

Strategies to inhibit HIF-1α pathways include pharmacological intervention of HIF-1α, genetic disruption of HIF-1α or blockade of hypoxia-inducible transcription [15]. PX-478 (S-2-amino-3-[4'-N,N,-bis(chloroethyl)amino]phenyl propionic acid N-oxide dihydrochloride) is a selective inhibitor that suppresses constitutive and hypoxia-induced HIF-1α levels [16]. PX-478 inhibits HIF-1α at multiple levels including inhibition of HIF-1α translation and reduction in HIF-1α mRNA levels [16]. Previous studies showed that PX-478 can enhance radiosensitivity and act synergistically with other anti-cancer drugs such as arsenic trioxide and gemcitabine [17-19]. However, as one of the hypoxic tumors, data about PX-478 in ESCC is few. In this study, we evaluate effects of HIF-1α, COX-2, PD-L1 expression on prognosis of ESCC patients and investigate the effect and the molecular mechanism of PX-478 in ESCC both in vitro and in vivo.

Materials and methods

Patients and tissue samples

Surgical specimens were collected from 133 patients with pT3N0M0 stage thoracic ESCC, as previously reported [20]. These tissues were obtained postoperatively between 2005-2013 from Shandong Cancer Hospital and Institute.

The Institutional Review Board approved the database and study design. Patients who received neoadjuvant therapy, adjuvant therapy or immunotherapy were excluded. Cases of in-hospital death were also excluded. The pathologic stage was determined according to the TNM classification system proposed by the AJCC (7th edition) [4]. Also, the histological features of the specimens were evaluated by two senior pathologists according to the WHO classification criteria. Overall survival (OS) was calculated from the date of primary surgical treatment until the date of death or last follow-up. The length of disease-free survival (DFS) was defined as the time between the primary surgical treatment and diagnosis of a recurrent tumor.

Cell culture and drug treatment

EC109 were kindly provided by Dr. Yufeng Cheng (Shandong University Qilu Hospital, Jinan, China). Both cell lines were cultured in RPMI 1640 (hyclone, USA) supplemented with 10% fetal bovine serum (FBS, Gibco) at 37°C in a 5% CO_2 humidified incubator (Thermo Fisher Scientific Inc., Waltham, MA, USA). Cells were starved for 24 h in medium containing 0.1% FBS prior to treatment, and then PX-478 (Selleck, Houston, USA) and $CoCl_2$ (Sigma-Aldrich Inc, St Louis, MO) was added to the cultures separately to a final concentration of 20 umol/L and 200 umol/L after serum starvation overnight.

Cell counting kit-8 (CCK-8) assay and cell proliferation curve

After CCK-8 (Bestbio, Shanghai, China) was used to make cell number standard curve according to the protocal, logarithmically growing EC109 cells and EC9706 cells were seeded in 96-well plates at a cell density of 5000/well. Each sample was seeded in four replicates. The medium was replaced at 2-day intervals. Viable cells were counted by the CCK-8 assay after 1, 2, 3, 4, and 5 days of growth. At different time intervals, the cells were incubated with CCK8 reagent for 1 hour at 37°C. OD of each well was measured at 450 nm using Thermo Scientific Varioskan Flash (Thermo Scientific, Finland). Cell numbers, mean values of three independent experiments, were used to make the proliferation curve.

Cell cycle analysis

Cells, treated with PX-478 in serum-free medium for 24 hours, were harvested and fixed in cold 75% ethanol, incubated with DNA as solution and stained with propidium iodide according to kit protocol (Bestbio, Beijing, China). Cells (10,000) were analyzed on a BD FACS Calibur cytometer using CellQuest Software (Becton Dickinson, San Diego, CA). Modifit LT 4.1 software was used to analyze the results.

Cell apoptosis analysis

Cells, treated with PX-478 in serum-free medium for 24 hours, were harvested and used to do cell flow cytometry of apoptosis with FITC Annexin V Apoptosis Detection Kit I (BD, USA). Wash cells twice with cold PBS and then resuspend cells in 1 × Binding Buffer at a concentration of 1×10^6 cells/ml. Transfer 100 µl of the solution (1×10^5 cells) to a 5 ml culture tube. Add 5 µl of FITC and 5 µl PI. Gently vortex the cells and incubate for 15 min at RT (25°C) in the dark. Add 400 µl of 1 × Binding Buffer to each tube. Analyze by flow cytometry within 1 hours. Results were analyzed with FCS express V3.

Lentivirus transfection assay

Lentivirus-mediated small interfering RNA delivery system was constructed using the sequence, 5'-TTCTCCGAACGTGTCACGT-3', made by GenePharma, Shanghai, China. The vector is LC3NC. Lentivirus was transfected using Enhanced Infection Solution with 5 µg/ml polybrene. After 12 h incubation, the transfection medium was changed into normal culturing medium with 10% FBS.

Western blotting

Whole cell protein extracts were prepared using Total Protein Extraction kit (Beyotime, Beijing, China), and protein concentration was determined by Bio-Rad protein assay (Bio-Rad). 20 µg of isolated protein was separated by 12% SDS-PAGE gel electroblotted onto a PVDF membrane. Then membranes were incubated overnight at 4°C with primary antibodies to β-actin (20536-1-p, proteintech, USA, 1:2000), HIF-1α (Abcam, UK; dilution 1:500), COX-2 (12282S, clone D5H5, CST, USA dilution 1:1000), PD-L1 (ab174838, clone EPR1161(2), Abcam, UK;

dilution 1:100), E-Cadherin (3195T, clone 24E10, CST USA dilution 1:1000), N-Cadherin (13116T, clone D4R1H, CST USA dilution 1:1000), Vimentin (5741T, clone D21H3, CST, USA dilution 1:1000), cleaved-caspase 3 (9953T, clone 5A1E, CST, USA dilution 1:1000), cleaved-PARP (5625T, clone D64E10, CST, USA dilution 1:1000), cyclin B1 (12231T, clone D5-C10, CST, USA dilution 1:1000) and P-histone H3 (4499T, clone D1H2, CST, USA dilution 1:1000). The membranes were then incubated with the appropriate HRP-conjugated secondary antibodies (CST, USA) for 1 hour at room temperature.

Quantitative real-time PCR (qRT-PCR)

Total RNA was isolated with TRIzol Reagent (Invitrogen, Carlsbad, CA, USA) and first strand cDNA was synthesized from 1 ug total RNA using ReveTra Ace qPCR Kit (TOYOBO, Japan). QRT-PCR was done using 2 ul of first-strand cDNA to quantitatively determine the relative amounts of cDNAs. Primers used were for COX-2: F, 5'-ATGCTGACTATGGCTACAAAAGC-3' and R, 5'-TCGGGCAATCATCAGGCAC-3'; PD-L1: F, 5'-TTGCTGAACGCCCCATACAA-3' and R, 5'-TCCAGATGACTTCGGCCTTG-3'; HIF-1α: F, 5'-GACGTCGAAAAGAAAAGTCTCG-3' and R, 5'-CCTTATCAAGATGCGAACTCACA-3'; β-actin: F, 5'-CATGTACGTTGCTATCCAGGC-3' and R, 5'-CTCCTTAATGTCACGCACGAT-3'. β-actin was used as internal control in all reactions. Real Time PCR reactions were carried out in triplicate in a volume of 25 µl containing 50 ng of cDNA template,1 × SYBR Green Mix (Toyobo, Japan), and 400 nM of forward and reverse primers. Samples were heated to 95°C for 1.5 min, followed by 40 amplification cycles for 30 sec at 95°C and for 30 sec at 65°C for annealing and amplification. Product purity was controlled by melting point analysis. The amount of mRNA was normalized to the endogenous reference β-actin.

Immunohistochemistry (IHC)

IHC analysis of HIF-1α, COX-2 and PD-L1 was performed using a standard technique, as previously reported [20]. Paraffin-embedded specimens were cut into 4 µm sections and baked at 65°C for 30 minutes. The sections were then processed by deparaffinization, rehydration through a series of graded ethanol, and then exposed to the antigen retrieval system under
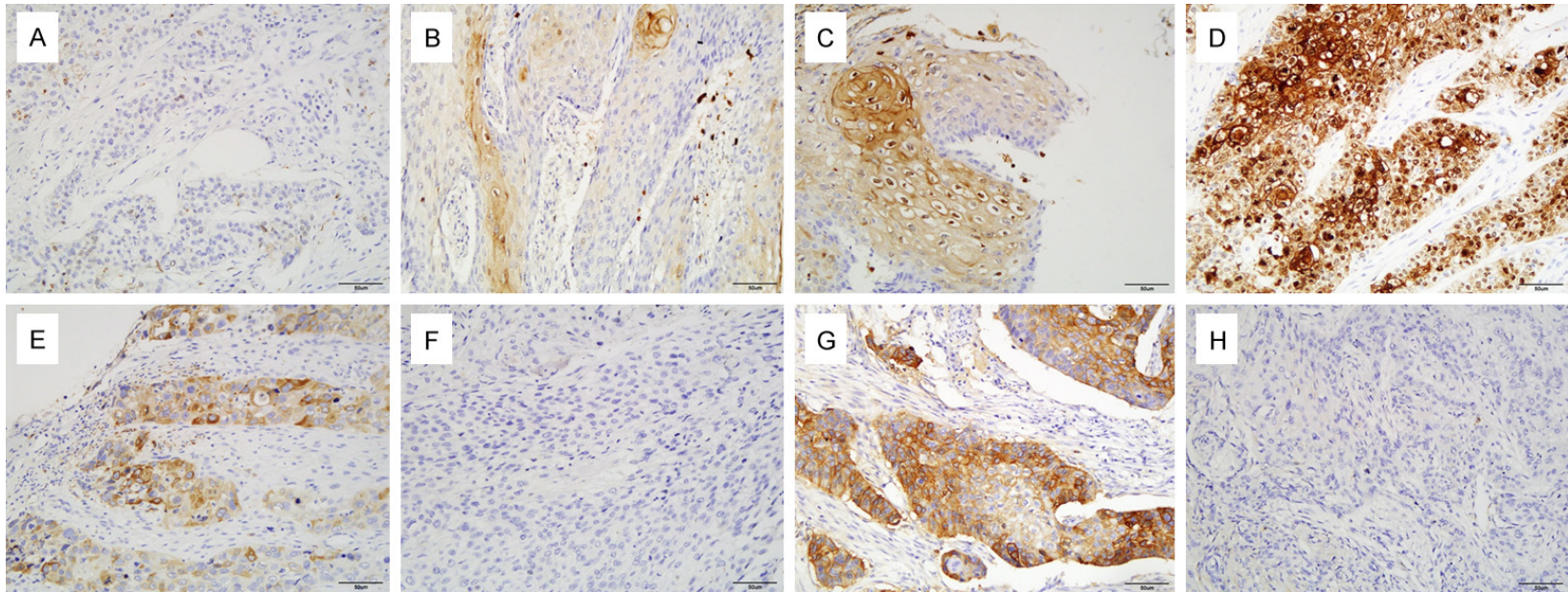
Figure 1. Representative pictures of IHC staining of HIF-1α (A, 0; B, 1+; C, 2+; D, 3+), COX-2 (E, Positive; F, Negative) and PD-L1 (G, Positive; H, Negative) in tissue sections of ESCC. COX-2 expression was primarily localized to the cytoplasm of cancer cells, while HIF-1α expression was observed in both cytoplasm and nucleus of cancer cells and PD-L1 expression in the cytoplasm and membrane of cancer cells.

Table 1. Association of HIF-1α, COX-2 and PD-L1 expression with known clinicopathological parameters

Parameters	No. patients	HIF-1α					COX-2			PD-L1		
		-	+	++	+++	P value	-	+	P value	-	+	P value
Age (years)						0.791			0.548			**0.029**
≤59	67	10	23	17	17		40	27		45	22	
>59	66	7	21	21	17		36	30		32	34	
Gender						0.345			0.686			0.361
Male	75	8	23	26	18		44	31		46	29	
Female	58	9	21	12	16		32	26		31	27	
Pre-op KPS						0.250			0.489			0.188
KPS≤80	89	12	28	22	27		49	40		48	41	
KPS>80	44	5	16	16	7		27	17		29	15	
Tumor location						0.159			0.272			0.801
Upper	23	2	6	5	10		10	13		12	11	
Middle	57	4	23	18	12		36	21		33	24	
Lower	53	11	15	15	12		30	23		32	21	
Tumor Length						0.254			0.292			**<0.001**
≤4 cm	70	9	25	23	13		43	27		51	19	
>4 cm	63	8	19	15	21		33	30		26	37	
Differential Grade						0.170			0.774			**0.002**
Well	46	8	21	8	9		28	18		32	14	
Moderate	53	6	15	18	14		30	23		34	19	
Poor	34	3	8	12	11		18	16		11	23	
Recurrence						**0.024**			0.104			**0.037**
No	23	7	9	3	4		17	6		18	5	
Yes	110	10	35	35	30		59	51		59	51	

KPS, Karnofsky performance score; HIF-1α, hypoxia-inducible factor-1α; COX-2, cyclooxygenase-2; PD-L1, programmed death-ligand 1. Bold values are statistically significant (P<0.05).

high pressure for two min. Slides were then exposed overnight at 4°C with the following primary antibodies: anti-HIF-1α (clone EP118, Beijing Zhongshan Golden Bridge Biotechnology Company, Beijing, China), anti-COX-2 (clone SP21, Beijing Zhongshan Golden Bridge Biotechnology Company, Beijing, China) and anti-PD-L1 (clone SP142, Beijing Zhongshan Golden Bridge Biotechnology Company). Secondary biotin-conjugated antibodies were used at 1:200. Five random fields were selected per section and analyzed under 400 × magnification. Immunostained sections were examined by two authors (Z. J. and Z. Y.) who were unaware of patient characteristics. Cases showing discrepancies were jointly reevaluated until consensus was reached. HIF-1α staining was assessed with the following scale: 0, nuclear staining in less than 1% of cells; 1+, nuclear staining in 1%-10% of cells and/or with weak cytoplasmic staining; 2+, nuclear staining in 10% to 50% of cells and/or with distinct cytoplasmic staining; 3+, nuclear staining in more than 50% of cells and/or with strong cytoplasmic staining. And then each specimen was categorized as low (0 and 1+) or high (2+ and 3+). The intensity of IHC reactions with COX-2 was appraised in a manner similar to that of a previous publication [21]: negative for no staining or the staining was present in only individual tumor cells (<10%), positive for the expression observed in tumor cells (>10%) or in numerous cell clumps. PD-L1 staining intensity was recorded in a way same as our previous publication [20]: negative for no staining, positive for membranous or cytoplasmic staining in tumor cells or lymphocytes.

Subcutaneous xenograft in nude mice

EC109 cells were re-suspended in PBS at 10^7/mL. A total of 12 BABL/c nude female, 18 ± 2 g,

Table 2. Correlation of immunohistochemical variables with each other

	HIF-1α	COX-2
COX-2		
r	0.416	
p	**<0.001**	
PD-L1		
r	0.382	0.277
p	**<0.001**	**0.001**

HIF-1α, hypoxia-inducible factor-1α; COX-2, cyclooxygenase-2; PD-L1, programmed death-ligand 1. Bold values are statistically significant (P<0.05).

SPF grade, were purchased from Nanjing Biomedical Research Institution of Nanjing University, Nanjing, China. The tumor xenograft was established by injecting EC109 cells in the right flank area of 6-week-old female BALB/c nude mice respectively. The 12 tumor-bearing mice in each group were randomly divided into two groups (6 mice for each group): the control group (isometric placebo) and the PX-478 groups (30 mg/kg every other day). All the drugs were delivered via p.o. gavage administration. Tumor size was determined with calipers in the long (L) and short (S) diameters every 3 days. The tumor volume was calculated by the following formula: Tumor volume was determined by external measurements with a caliper and calculated as $V = L \times S^2 \times 0.5$. Animal care was provided according to institutional guidelines. Tumors were harvested after 19 days. All animal experiments were undertaken in accordance with the NIH Guide for the Care and Use of Laboratory Animals, with the approval of the Committee on the Use and Care of Animals in Shandong University.

Statistical analysis

The data represent mean ± SD from three independent experiments. Standard error bars were included for all data points. The data were then analyzed using Student's t test when only two groups were present or assessed by one-way analysis of variance (ANOVA) when more than two groups were compared. Kaplan-Meier's statistics and log-rank tests were performed to estimate the significance of differences in survival times. A multivariate survival analysis was performed using Cox proportional hazards regression modeling. In the multivariate analysis, all variables that were associated significantly with patient survival in the univariate analysis were included in the final analysis. Statistical analysis was performed using SPSS software (version 17.0; SPSS, Inc., Chicago, IL). Data were considered significant if P<0.05.

Results

Association of HIF-1α, COX-2, PD-L1 expression with clinicohistopathologic features and clinical outcome

Staining results for HIF-1α, COX-2 and PD-L1 in 133 ESCC with pathological stage T3N0M0 are shown in **Figure 1**. HIF-1α expression was observed in both cytoplasm and nucleus of cancer cells, while positive immunostaining for COX-2 occurred in a cytoplasmic localization and PD-L1 expression was observed in the cytoplasm and membrane of cancer cells (**Figure 1**). As shown in **Table 1**, positive PD-L1 expression was significantly correlated with older age (>59 versus ≤59, P=0.029), poorer histological differentiation (P=0.002) and longer tumor length (>4 cm versus ≤4 cm, P<0.001). Moreover, there was a statistically significant correlation between tumor recurrence and HIF-1α, PD-L1 expression (**Table 1**, P=0.024 and 0.037, respectively).

Based on our IHC staining scores, HIF-1α, COX-2 and PD-L1 was overexpressed in 54.13% (72/133), 42.86% (57/133) patients and 42.1% (52/133), respectively. There was a moderate significant correlation between HIF-1α and COX-2 expression in these samples (**Table 2**, r=0.416, P<0.001). Also, a slight positive correlation between PD-L1 and HIF-1α expression as well as PD-L1 and COX-2 expression (**Table 2**, r=0.382, P<0.001 and r=0.277, P=0.001 respectively).

Similar to previous studies [8, 10, 20, 22], ESCC samples expressing high levels of HIF-1α, COX-2 and PD-L1 were associated with unfavorable DFS (P=0.004, 0.046 and 0.002; respectively; Supplementary Figure 1A-C) and OS (P=0.003, 0.033, 0.001; respectively; Supplementary Figure 1D-F). In multivariate analysis, HIF-1α and PD-L1 expression, as well as KPS status were correlated independently with DFS (P=0.033, 0.044 and 0.043, respectively) and OS (P=0.027, 0.039 and 0.031, respectively) when considering tumor differentiation and COX-2 expression (**Table 3**). In addition, patients with positive PD-L1 expression along with higher COX-2 expression had worst

Table 3. Univariable and multivariable analyses of predictors of disease-free survival and overall survival

Variable	Disease-Free Survival				Overall Survival			
	Univariable Analysis		Multivariable Analysis		Univariable Analysis		Multivariable Analysis	
	HR (95% CI)	P	HR (95% CI)	P	HR (95% CI)	P	HR (95% CI)	P
Age (≤60 vs. >60)	1.046 (0.719-1.521)	0.814			1.033 (0.691-1.545)	0.874		
Gender (male vs. female)	1.203 (0.824-1.755)	0.338			1.241 (0.828-1.860)	0.295		
Pre-op KPS (<80 vs. ≥80)	0.622 (0.413-0.936)	**0.023**	0.652 (0.431-0.986)	**0.043**	0.607 (0.388-0.949)	**0.029**	0.609 (0.387-0.956)	**0.031**
Tumor location								
Upper	Ref.	0.502			Ref.	0.135		
Middle	0.827 (0.489-1.339)	0.479			0.956 (0.546-1.673)	0.875		
Lower	0.730 (0.430-1.239)	0.243			0.632 (0.353-1.131)	0.122		
Tumor length (≤4 cm vs. >4 cm)	0.874 (0.600-1.272)	0.481			0.929 (0.620-1.393)	0.722		
Differential grade								
Well	Ref.	**0.046**	Ref.	0.418	Ref.	0.095	Ref.	0.601
Moderate	1.394 (0.890-2.183)	0.147	1.249 (0.785-1.987)	0.348	1.396 (0.859-2.270)	0.179	1.232 (0.746-2.033)	0.415
Poor	1.847 (1.136-3.005)	**0.013**	1.419 (0.833-2.419)	0.198	1.785 (1.055-3.020)	**0.031**	1.315 (0.745-2.322)	0.345
IHC markers								
HIF-1α (low vs. high)	1.760 (1.198-2.588)	**0.004**	1.559 (1.037-2.344)	**0.033**	1.869 (1.232-2.837)	**0.003**	1.658 (1.060-2.593)	**0.027**
COX-2 (low vs. high)	1.467 (1.006-2.138)	**0.046**	1.269 (0.854-1.887)	0.239	1.550 (1.035-2.320)	**0.033**	1.305 (0.856-1.989)	0.216
PD-L1 (negative vs. positive)	1.845 (1.262-2.698)	**0.002**	1.518 (1.012-2.276)	**0.044**	1.957 (1.303-2.939)	**0.001**	1.582 (1.023-2.447)	**0.039**

KPS, Karnofsky performance score; HIF-1α, hypoxia-inducible factor-1α; COX-2, cyclooxygenase-2; PD-L1, programmed death-ligand 1. Bold values are statistically significant (P<0.05).
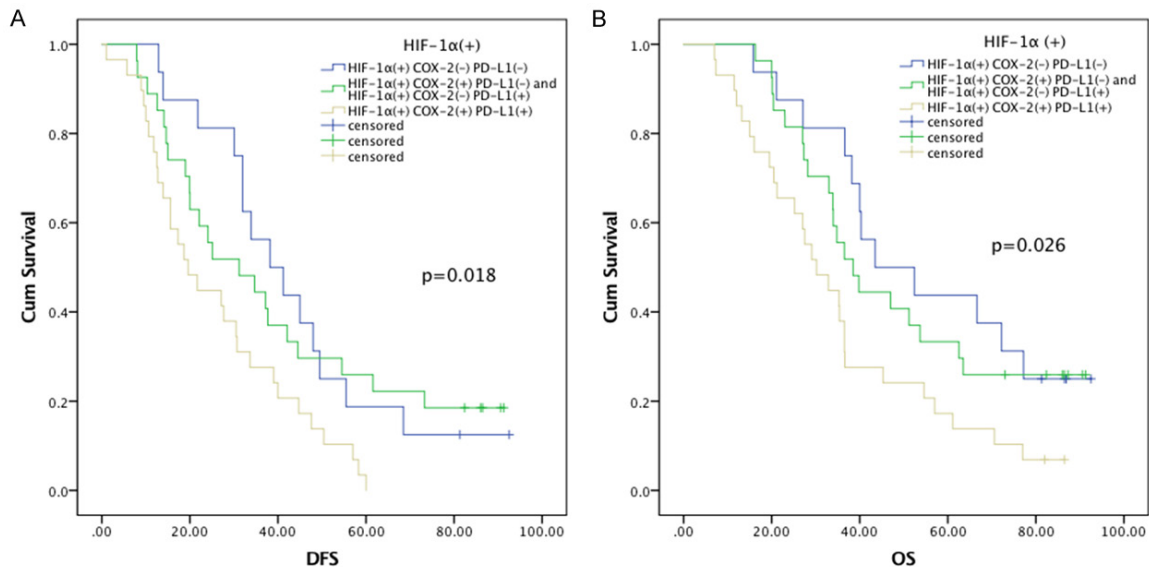

Figure 2. Subgroups with higher COX-2 and positive PD-L1 expression had the worst DFS (A) and OS (B) in ESCC patients with higher HIF-1α expression (2+ and 3+).

DFS (P=0.018) and OS (P=0.026) in the subgroup of patients with high level HIF-1α expression (**Figure 2A** and **2B**).

HIF-1α expression and effects of PX-478 treatment on HIF-1α, COX-2, and PD-L1 protein expression in EC109 and EC9706

To determine the role of HIF-1α and its antagonism by PX-478 in ESCC, we evaluated HIF-1α, COX-2 and PD-L1 expression levels in a panel of ESCC cell lines in vitro under normoxic or hypoxia-mimicking conditions (CoCl$_2$ treatment) and transfected with HIF-1α knockdown or control shRNA by Western blot and real-time PCR. As shown in **Figure 3A-F**, when HIF-1α expression was knocked down with shRNA, COX-2 and PD-L1 mRNA expressions were decreased significantly in both EC109 (P<0.05 for both) and EC9706 (P<0.01 and P<0.0001, respectively).
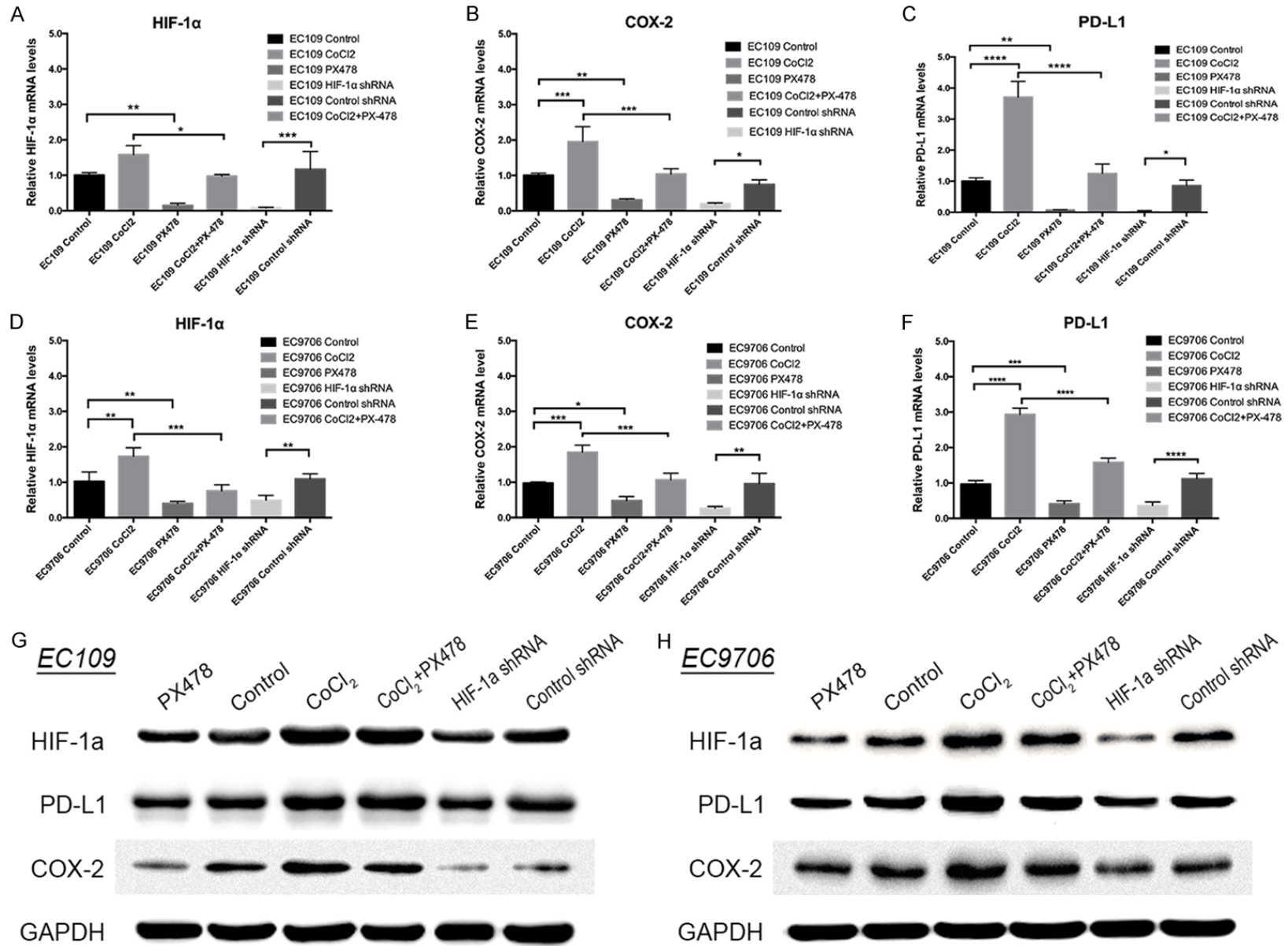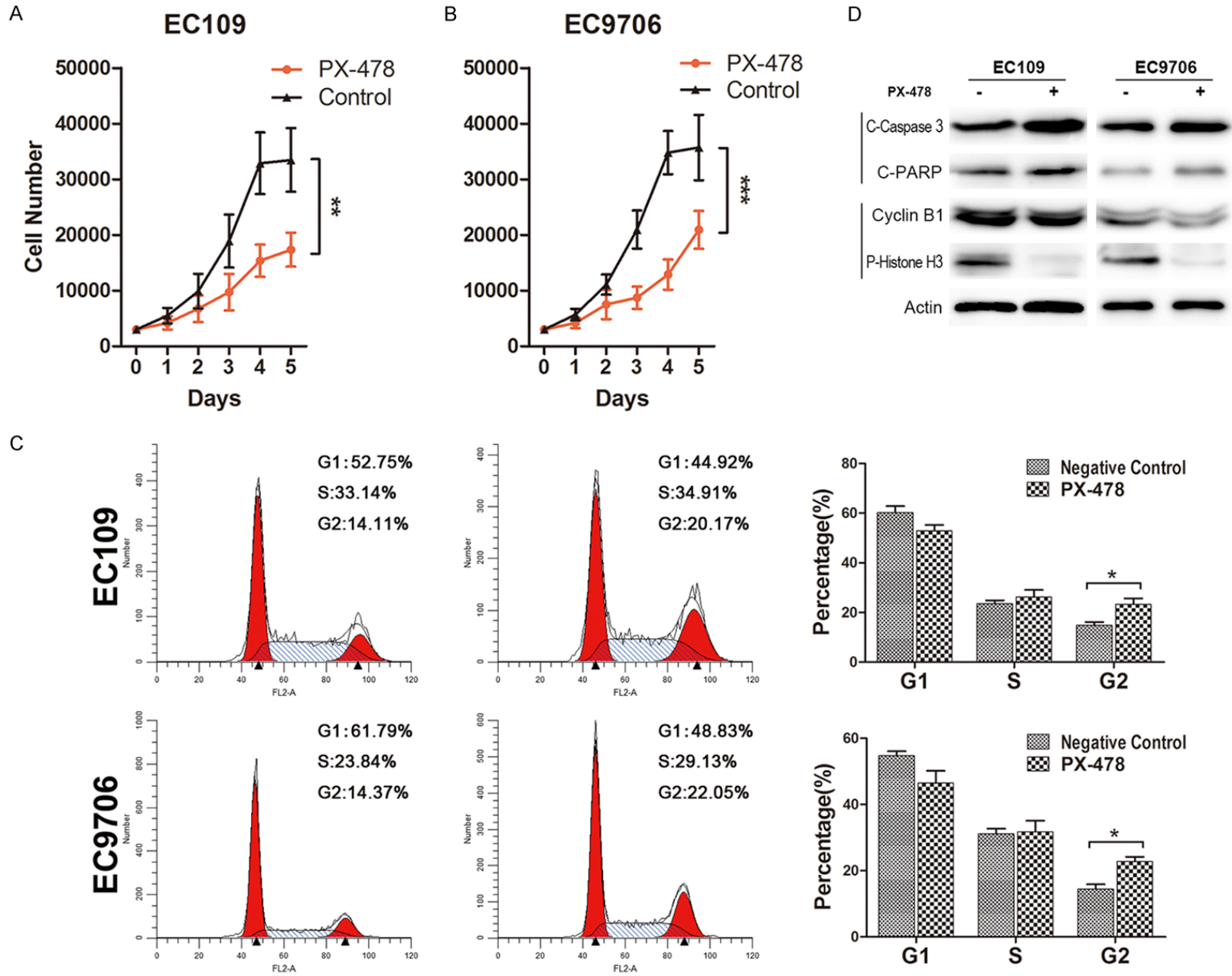
Figure 3. The mRNA and protein levels of HIF-1α, COX-2 and PD-L1 in $CoCl_2$ treatment group, PX-478 treatment group, PX-478 and $CoCl_2$ treatment group, HIF-1α shRNA group, control shRNA group and control group. *P≤0.05; **P≤0.01; ***P≤0.001; ****P≤0.0001.
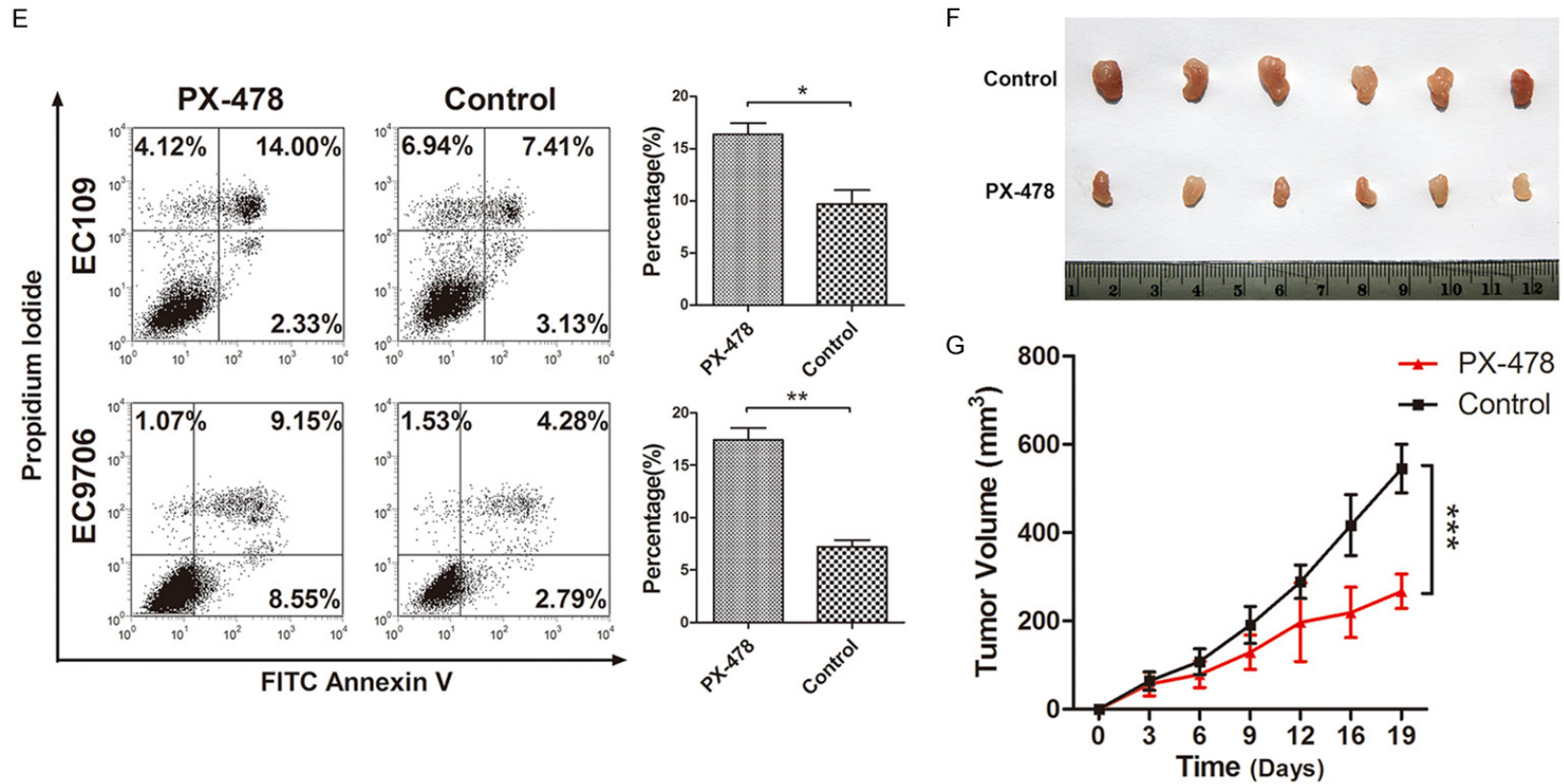
Figure 4. The effect of PX-478 on cell proliferation, cell cycle distribution and apoptosis in EC109 and EC9706 cell lines. PX-478 inhibited cell proliferation. Cell numbers of EC109 (A) and EC9706 (B) treated with PX-478 or without any treatment were monitored for 5 days. Data were mean ± SD. ***P<0.001. Representative figures of cell cycle detection by PI staining using flow cytometry. Numbers were percentage of corresponding phases. *P≤0.05 (C). Both cell lines were treated with 20 μM PX-478 that induced both a decrease in G2 phase-related protein expression (e.g., cyclin B1 and P-Histone H3) as well as an increase in apoptosis proteins (e.g., cleaved-caspase 3 and cleaved-PARP) (D). PX-478 induced higher percentage of EC109 and EC9706 cell apoptosis. Cell apoptosis was detected by Annexin V and PI staining. *P≤0.05; **P≤0.01 (E). ESCC cell line EC109 was inoculated into the right flank of the nude nu/nu mice (6 mice/group), and subsequently treated with placebo (control) and HIF-1α inhibitor (PX-478) (p.o. gavage at 30 mg/kg, every other day). Representative image of tumors in nude mice (F). Time-dependent tumor growth of treated groups was analyzed by two-way ANOVA by comparison with the untreated group. PX-478 treated group was compared with control group. The data of all primary tumors were expressed as mean ± SD. *P<0.05, **P<0.01, ***P<0.001 (G).
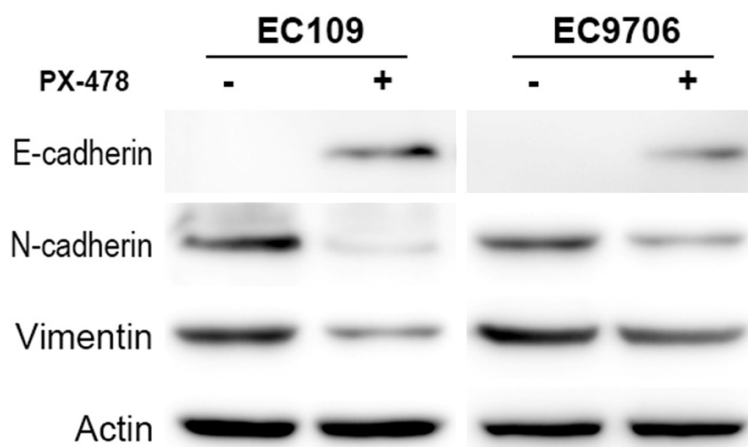
Figure 5. PX-478 inhibits EMT of ESCC. Expression levels of Vimentin and N-cadherin were decreased while E-cadherin was increased in the PX-478 treatment group.

Figure 3C, PX-478 treatment resulted in G2/M arrest with more cells in G2 phase compared with the control. In EC109, the percentage of G2 cells increased significantly from 14.81% to 23.31% (P= 0.0362). Changes were similar in EC9706 14.43% to 22.78% (P=0.0148, **Figure 4C**). Furthermore, changes of G2/M related proteins by western blot verified the inhibition of G2/M transition after PX-478 treatment. Cyclin B, which is necessary for G2/M transition, was downregulated after PX-478 treatment (**Figure 4D**). Meanwhile, significantly decreased phosphorylated histone H3 was observed after PX-478 treatment, which indicated fewer cells were in mitotic phase (**Figure 4D**). In addition, we performed an Annexin V-FITC/PI double-staining assay to explore the apoptosis changes. Increased proportions of apoptotic cells (including early and late apoptotic cells) were observed in PX-478 treatment cells from 9.71% to 16.38% in EC109 (P=0.0173) and 7.19% to 17.40% EC9706 (P=0.0015, **Figure 4E**). Consistent with the above results, western blot showed PX-478 induced the expression of apoptotic markers (cleaved-caspase 3 and cleaved-PARP) (**Figure 4D**).

In the meantime, 12 nude mice were subcutaneously inoculated with ESCC cells. Compared to the normal saline injected group, PX-478 did inhibit the growth of the tumor (P<0.001, **Figure 4F** and **4G**), suggesting that PX-478 is a potential and promising strategy in the treatment of ESCC.

Epithelial-mesenchymal transition (EMT) was inhibited in EC109 and EC9706 cells after PX-478 treatment

EMT has been accepted as a necessary step of metastasis [23]. An important evidence for EMT is the change of characteristic phenotypic markers. The "cadherin switch" from E-Cadherin to mesenchymal neural cadherin (N-cadherin) alters cell adhesion [24]. Gain of vimentin expression is also a sign of "complete EMT" [25]. Here, we observed the expression

Besides, when HIF-1α expression was upregulated in CoCl$_2$ group, COX-2 and PD-L1 mRNA expressions were elevated greatly compared to the control group in EC109 (P<0.001 and P<0.0001, respectively) and EC9706 (P<0.001 and P<0.0001, respectively). The protein expression of COX-2 and PD-L1 showed the similar change (**Figure 3G** and **3H**). We then incubated the EC9706 and EC109 cell lines, with the HIF-1α antagonist PX-478 under normoxic or hypoxia-mimicking conditions and measured HIF-1α, COX-2 and PD-L1 levels by RT-PCR and Western blot analysis. As shown in **Figure 3G** and **3H**, PX-478 inhibited normoxic and hypoxia-induced HIF-1α expression as well as COX-2 and PD-L1 expression in vitro at a dose of 20 μM in EC9706 and EC109 cells. RT-PCR showed the similar results (**Figure 3A-F**). Together, these data demonstrate that HIF-1α is involved in COX-2 and PD-L1 expression. Targeted HIF-1α can effectively reduce their expression.

PX-478 inhibits tumor growth via inhibiting G2/M transition and inducing apoptosis of EC109 and EC9706

As shown in **Figure 3A** and **3B**, both cell lines had significantly decreased proliferation rate after PX-478 treatment for 5 days (P<0.001 for both, **Figure 4A** and **4B**). To further evaluate the mechanism underlying the inhibited proliferation, PI staining for flow cytometry was used to detect cell cycle change in EC109 and EC9706 cells after PX-478 treatment. As shown in

levels of E-cadherin, Vimentin and N-cadherin with specific antibodies. Western blot also showed that E-cadherin protein expression significantly increased whereas Vimentin and N-cadherin decreased in response to PX-478 treatment, which indicates a reversed EMT transition happened (**Figure 5**).

Discussion

In our study, we demonstrated the overexpression of HIF-1α and its associated factor COX-2, and PD-L1 were correlated to poor prognosis in ESCC. Furthermore, patients with PD-L1 and COX-2 overexpression had worst survival in subgroup of patients with high HIF-1α expression. PX-478, the selective HIF-1α inhibitor, has a wide effect on tumor development, such as suppressing proliferation, inhibiting EMT process, arresting cell cycle and promoting cells apoptosis. In vivo mouse xenograft models also showed the inhibitory effect on tumor growth. Moreover, it can reduce the inflammatory molecule COX-2 and immunosuppressive molecule PD-L1 expression.

HIF-1α is a pivotal regulatory factor that enables tumor cells to adapt to hypoxic microenvironment by binding to specific DNA sequences in the promoters of a number of genes including COX-2 and PD-L1 in conditions of low oxygen tension [5, 9, 11, 12]. COX-2 and PD-L1 has been regarded as important molecules involved in cancer inflammation and immune evasion respectively [13, 26]. It has been reported that overexpression of COX-2 in ESCC correlates with depth of invasion, TNM stage and reduced OS [10]. PD-1/PD-L1 circuit is important in regulating immune tolerance by inhibiting T or B cell activation [13]. Studies have reported PD-L1 may be associated poorer recurrence-free survival and OS [20, 22, 27]. Our clinical analysis showed that HIF-1α was associated with COX-2 and PD-L1 expression as well as prognosis of ESCC patients and patients with high expression of all those three molecular had poorer survival than other patients in patients with the same TNM stage (pT3N0M0). We also validate the association by treatment with CoCl$_2$, which can block the HIF-1α degradation and increase HIF-1α expression in a dose-dependent manner [28, 29], and shRNA to knockdown the HIF-1α gene. We found hypoxia promotes COX-2 and PD-L1 expression through a HIF-1α-dependent mech-

anism in ESCC cells. Based on those data, selective inhibition of HIF-1α may have a broader range of therapeutic effect than targeting of downstream factors due to the more comprehensive direct and indirect effects of HIF-1 blockade on tumor cells.

Although the function of HIF-1α such as in ESCC has been well-studied, few researches about HIF-1α inhibitors has been done in ESCC. Among increasing number of putative small molecule inhibitors of HIF-1α, only a few are progressing through preclinical and early clinical development, of which PX-478 is a selective HIF-1α inhibitor and suppresses constitutive and hypoxia-induced levels of HIF-1a in cancer cells [15, 30]. Previous studies have shown PX-478 can enhance radiosensitivity of prostate cancer cells and sensitizes pancreatic tumor xenografts to radiation therapy [19]. Moreover, Lang et al. [17] reported that PX-478, acts synergistically with arsenic trioxide leading to a more efficient reactive oxygen species (ROS)-induced apoptosis in pancreatic tumor xenografts models. So far, data about PX-478 in ESCC is scarce. Our data exhibited PX-478 can inhibit tumor growth both in vitro and in vivo. Moreover, at the cellular level, PX-478 can promote apoptosis and inhibit G2/M transition. Also, the shift from vimentin, N-cadherin to E-cadherin, suggested that PX-478 did repress EMT events in ESCC cells. Taken together, PX-478 has a comprehensive and wide effect on the tumor including the promotion of tumor inflammation, decrease of tumor immunosuppression and inhibition of tumor cell proliferation. Therefore, it is a viable and important candidate for anti-cancer therapy of ESCC.

Recent studies showed that PX-478 can provide an immune adjuvant activity [18, 31]. In pancreatic ductal adenocarcinoma, PX-478 can enhance the anti-tumor effect of gemcitabine by inducing immunogenic cell death [18]. Also, it improves the efficacy of tumor antigen-based dendritic cell vaccine in a mouse model of breast cancer [31]. Similar to the above results, we found PX-478 can reduce the expression of PD-L1 through reduction of HIF-1α expression in vitro, which suggests PX-478 may be a possible therapeutic approach to break down the immunosuppressive regulatory network of tumor microenvironment. Also, we found PX-478 can significantly reduce COX-2 expres-

sion, which may exhibit the similar role of aspirin in modulation of inflammation. Since aspirin is recommended for the prevention of colorectal cancer, based on the above results, PX-478 may be a promising therapeutic strategy to treat patients with solid tumors [32, 33]. Also, in our survival analysis, patients with high COX-2 and PD-L1 expression had poorer survival. Since PX-478 may suppress COX-2 and PD-L1 expression through inhibiting HIF-1α expression, PX-478 may be an important candidate for anti-cancer therapy of these patients. However, the inter-related anticancer mechanisms of PX-478 need to be clarified in future studies.

In recent years, the discovery and development of novel small molecules targeting HIF-1α has been an exciting area of developmental therapeutics that has grown exponentially [15, 30]. The main challenge of these small molecule HIF-1α inhibitors is the specificity [15, 30]. So far, none of the presently available inhibitors appears to disrupt the HIF-1α pathway as their exclusive target [15]. Compared to other agents have been reported to lower HIF-1α protein levels such as camptothecins, phosphatidylinositol 3-kinase inhibitors, YC-1, histone deacetylase inhibitors, heat shock protein 90 inhibitors and microtubule cytoskeleton disrupting agents, PX-478 is more selective for lowering HIF-1α and is the only agent clearly shown to act at multiple levels through inhibition of HIF-1α transcription, translation and deubiquitination, which is independently of oxygen, von Hippel-Lindau protein, or p53 [15, 16, 30]. Thus, PX-478 may have less side effects than other agents. Since tumor hypoxia has been recognized as a common feature of solid tumors, the potent antitumor activity of PX-478 against HIF-1α-overexpressing tumors may be widely adopted in various kinds of tumors like immunotherapy.

In conclusion, our results suggested that a potential prognostic value for HIF-1α, COX-2 and PD-L1 in ESCC, as reflected by the correlation between high expression levels with poor outcomes. Also, the selective HIF-1α inhibitor PX-478 inhibited tumor growth both in vitro and in vivo, induced cell cycle arrest in G2 stage, promoted apoptosis and reduced COX-2 and PD-L1 expression of ESCC cells. As a selective HIF-1α inhibitor, the potent antitumor activity and ability to modulate inflammation and immune system could be useful as therapeutic candidates for the treatment of various diseases associated with over-activation of HIF-1α. Future research is warranted to further identify mechanisms in detail and to translate these developments into clinical trials.

Disclosure of conflict of interest

None.

Abbreviations

AJCC, American Joint Committee on Cancer; CCK-8, Cell counting kit-8; DFS, Disease-free survival; EC, Esophageal cancer; EMT, Epithelial-mesenchymaltransition; ESCC, Esophageal squamous cell cancer; HIF-1, Hypoxia-inducible factor-1; HIF-1α, Hypoxia-inducible factor-1 α-subunit; HIF-1β, Hypoxia-inducible factor-1 β-subunit; IHC, Immunohistochemistry; OS, Overall survival; PD-1, Programmed death 1; PD-L1, Programmed death ligand-1; pT3N0M0, Pathological stage T3N0M0.

Address correspondence to: Dr. Jinming Yu, Department of Radiation Oncology, Shandong Cancer Hospital and Institute, Shandong University, 440 Jiyan Road, Jinan 250117, Shandong, China. Tel: +86-531-87984729; Fax: +86-531-87984079; E-mail: yujinmingsd@126.com

References

[1] Chen W, Zheng R, Baade PD, Zhang S, Zeng H, Bray F, Jemal A, Yu XQ and He J. Cancer statistics in China, 2015. CA Cancer J Clin 2016; 66: 115-132.
[2] Rustgi AK and El-Serag HB. Esophageal carcinoma. N Engl J Med 2014; 371: 2499-2509.
[3] Jemal A, Siegel R, Xu J and Ward E. Cancer statistics, 2010. CA Cancer J Clin 2010; 60: 277-300.
[4] Rice TW, Blackstone EH and Rusch VW. 7th edition of the AJCC Cancer Staging Manual: esophagus and esophagogastric junction. Ann Surg Oncol 2010; 17: 1721-1724.

[5] Majmundar AJ, Wong WJ and Simon MC. Hypoxia-inducible factors and the response to hypoxic stress. Mol Cell 2010; 40: 294-309.

[6] Wang GL, Jiang BH, Rue EA and Semenza GL. Hypoxia-inducible factor 1 is a basic-helix-loop-helix-PAS heterodimer regulated by cellular O2 tension. Proc Natl Acad Sci U S A 1995; 92: 5510-5514.

[7] Talks KL, Turley H, Gatter KC, Maxwell PH, Pugh CW, Ratcliffe PJ and Harris AL. The expression and distribution of the hypoxia-inducible factors HIF-1alpha and HIF-2alpha in normal human tissues, cancers, and tumor-associated macrophages. Am J Pathol 2000; 157: 411-421.

[8] Ping W, Sun W, Zu Y, Chen W and Fu X. Clinicopathological and prognostic significance of hypoxia-inducible factor-1alpha in esophageal squamous cell carcinoma: a meta-analysis. Tumour Biol 2014; 35: 4401-4409.

[9] Kaidi A, Qualtrough D, Williams AC and Paraskeva C. Direct transcriptional up-regulation of cyclooxygenase-2 by hypoxia-inducible factor (HIF)-1 promotes colorectal tumor cell survival and enhances HIF-1 transcriptional activity during hypoxia. Cancer Res 2006; 66: 6683-6691.

[10] Li L, Zhao J, Wu Z, Wang G and Chen G. Meta-analysis: clinicopathological and prognostic significance of cyclooxygenase-2 expression on oesophageal squamous cell carcinoma. Aliment Pharmacol Ther 2009; 30: 589-596.

[11] Ruf M, Moch H and Schraml P. PD-L1 expression is regulated by hypoxia inducible factor in clear cell renal cell carcinoma. Int J Cancer 2016; 139: 396-403.

[12] Barsoum IB, Smallwood CA, Siemens DR and Graham CH. A mechanism of hypoxia-mediated escape from adaptive immunity in cancer cells. Cancer Res 2014; 74: 665-674.

[13] Ostrand-Rosenberg S, Horn LA and Haile ST. The programmed death-1 immune-suppressive pathway: barrier to antitumor immunity. J Immunol 2014; 193: 3835-3841.

[14] Wu P, Wu D, Li L, Chai Y and Huang J. PD-L1 and survival in solid tumors: a meta-analysis. PLoS One 2015; 10: e0131403.

[15] Xia Y, Choi HK and Lee K. Recent advances in hypoxia-inducible factor (HIF)-1 inhibitors. Eur J Med Chem 2012; 49: 24-40.

[16] Koh MY, Spivak-Kroizman T, Venturini S, Welsh S, Williams RR, Kirkpatrick DL and Powis G. Molecular mechanisms for the activity of PX-478, an antitumor inhibitor of the hypoxia-inducible factor-1alpha. Mol Cancer Ther 2008; 7: 90-100.

[17] Lang M, Wang X, Wang H, Dong J, Lan C, Hao J, Huang C, Li X, Yu M, Yang Y, Yang S and Ren H. Arsenic trioxide plus PX-478 achieves effective treatment in pancreatic ductal adenocarcinoma. Cancer Lett 2016; 378: 87-96.

[18] Zhao T, Ren H, Jia L, Chen J, Xin W, Yan F, Li J, Wang X, Gao S, Qian D, Huang C and Hao J. Inhibition of HIF-1alpha by PX-478 enhances the anti-tumor effect of gemcitabine by inducing immunogenic cell death in pancreatic ductal adenocarcinoma. Oncotarget 2015; 6: 2250-2262.

[19] Palayoor ST, Mitchell JB, Cerna D, Degraff W, John-Aryankalayil M and Coleman CN. PX-478, an inhibitor of hypoxia-inducible factor-1alpha, enhances radiosensitivity of prostate carcinoma cells. Int J Cancer 2008; 123: 2430-2437.

[20] Zhu Y, Li M, Mu D, Kong L, Zhang J, Zhao F, Li Z, Liu X, Bo C and Yu J. CD8+/FOXP3+ ratio and PD-L1 expression associated with survival in pT3N0M0 stage esophageal squamous cell cancer. Oncotarget 2016; 7: 71455-71465.

[21] Surowiak P, Materna V, Matkowski R, Szczuraszek K, Kornafel J, Wojnar A, Pudelko M, Dietel M, Denkert C, Zabel M and Lage H. Relationship between the expression of cyclooxygenase 2 and MDR1/P-glycoprotein in invasive breast cancers and their prognostic significance. Breast Cancer Res 2005; 7: R862-870.

[22] Chen MF, Chen PT, Chen WC, Lu MS, Lin PY and Lee KD. The role of PD-L1 in the radiation response and prognosis for esophageal squamous cell carcinoma related to IL-6 and T-cell immunosuppression. Oncotarget 2016; 7: 7913-7924.

[23] Yao D, Dai C and Peng S. Mechanism of the mesenchymal-epithelial transition and its relationship with metastatic tumor formation. Mol Cancer Res 2011; 9: 1608-1620.

[24] Lamouille S, Xu J and Derynck R. Molecular mechanisms of epithelial-mesenchymal transition. Nat Rev Mol Cell Biol 2014; 15: 178-196.

[25] Grunert S, Jechlinger M and Beug H. Diverse cellular and molecular mechanisms contribute to epithelial plasticity and metastasis. Nat Rev Mol Cell Biol 2003; 4: 657-665.

[26] Simmons DL, Botting RM and Hla T. Cyclooxygenase isozymes: the biology of prostaglandin synthesis and inhibition. Pharmacol Rev 2004; 56: 387-437.

[27] Ito S, Okano S, Morita M, Saeki H, Tsutsumi S, Tsukihara H, Nakashima Y, Ando K, Imamura Y, Ohgaki K, Oki E, Kitao H, Mimori K and Maehara Y. Expression of PD-L1 and HLA Class I in esophageal squamous cell carcinoma: prognostic factors for patient outcome. Ann Surg Oncol 2016; 23 Suppl 4: 508-515.

[28] Chandel NS, Maltepe E, Goldwasser E, Mathieu CE, Simon MC and Schumacker PT. Mitochondrial reactive oxygen species trigger hypoxia-induced transcription. Proc Natl Acad Sci U S A 1998; 95: 11715-11720.

[29] Guo M, Song LP, Jiang Y, Liu W, Yu Y and Chen GQ. Hypoxia-mimetic agents desferrioxamine

and cobalt chloride induce leukemic cell apoptosis through different hypoxia-inducible factor-1alpha independent mechanisms. Apoptosis 2006; 11: 67-77.

[30] Masoud GN and Li W. HIF-1alpha pathway: role, regulation and intervention for cancer therapy. Acta Pharm Sin B 2015; 5: 378-389.

[31] Kheshtchin N, Arab S, Ajami M, Mirzaei R, Ashourpour M, Mousavi N, Khosravianfar N, Jadidi-Niaragh F, Namdar A, Noorbakhsh F and Hadjati J. Inhibition of HIF-1alpha enhances anti-tumor effects of dendritic cell-based vaccination in a mouse model of breast cancer. Cancer Immunol Immunother 2016; 65: 1159-1167.

[32] Drew DA, Chin SM, Gilpin KK, Parziale M, Pond E, Schuck MM, Stewart K, Flagg M, Rawlings CA, Backman V, Carolan PJ, Chung DC, Colizzo FP 3rd, Freedman M, Gala M, Garber JJ, Huttenhower C, Kedrin D, Khalili H, Kwon DS, Markowitz SD, Milne GL, Nishioka NS, Richter JM, Roy HK, Staller K, Wang M and Chan AT. ASPirin Intervention for the REDuction of colorectal cancer risk (ASPIRED): a study protocol for a randomized controlled trial. Trials 2017; 18: 50.

[33] Drew DA, Cao Y and Chan AT. Aspirin and colorectal cancer: the promise of precision chemoprevention. Nat Rev Cancer 2016; 16: 173-186.

Inhibition of HIF-1α by PX-478 in ESCC
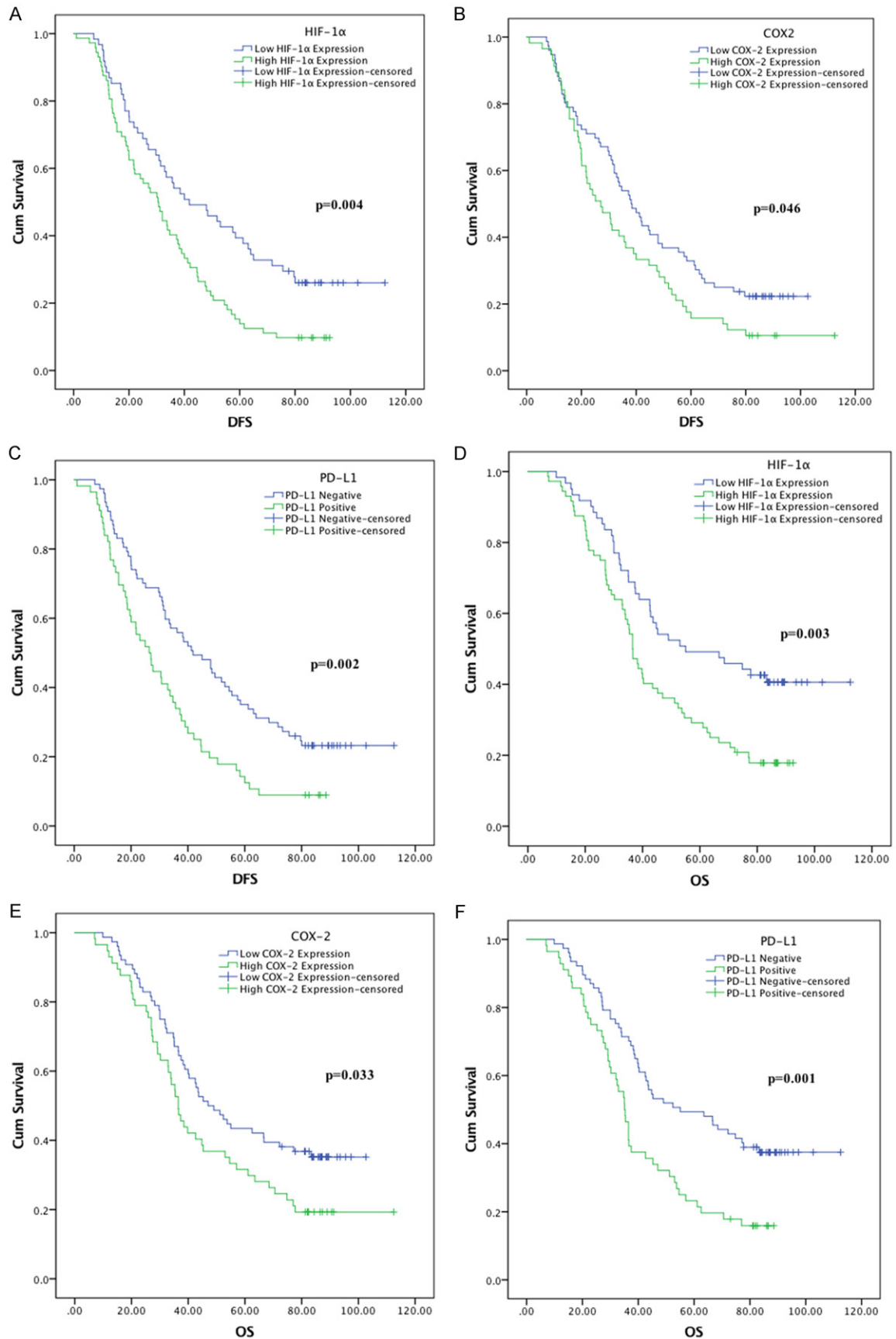
Supplementary Figure 1. Tumor HIF-1α, COX-2 and PD-L1 expression in ESCC is correlated with worse disease-free survival (A-C) and overall survival (D-F).